Basic data visualization in vintage seismic profiles: indications for the interpretation of the ViDEPI database (offshore Puglia, southern Italy)

Marianna Cicala[1], Domenico Chiarella[2], Francesco De Giosa[3] & Vincenzo Festa[1]

[1] Dipartimento di Scienze della Terra e Geoambientali, Università degli Studi di Bari “Aldo Moro”, via E. Orabona 4, 70125 Bari, Italy.
[2] Clastic Sedimentology Investigation (CSI), Department of Earth Sciences, Royal Holloway, University of London, Egham, Surrey, TW20 0EX, UK.
[3] Environmental Surveys S.r.l. (ENSU), Spin-Off dell’Università degli Studi di Bari “Aldo Moro”, 74123 Taranto, Italy.

MC, 0000-0001-7989-8877; DC, 0000-0003-2482-0081; VF, 0000-0001-6054-5035.

Rend. Online Soc. Geol. It., Vol. 59 (2023), pp. 56-63, 4 figs. https://doi.org/10.3301/ROL.2023.09

Short Note

Corresponding author e-mail: vincenzo.festa@uniba.it

Citation: Cicala M., Chiarella D., De Giosa F. & Festa V. (2023) - Basic data visualization in vintage seismic profiles: indications for the interpretation of the ViDEPI database (offshore Puglia, southern Italy). Rend. Online Soc. Geol. It., 59, 56-63, https://doi.org/10.3301/ROL.2023.09.

Guest Editor: Luigi Spalluto

Submitted: 12 October 2022
Accepted: 30 November 2022
Published online: 13 December 2022

ABSTRACT

The Visibility of Petroleum Exploration Data in Italy (ViDEPI) project represents a freely accessible valuable resource for the research community. However, seismic profiles available from this project present several limitations because information such as the basic shape of the seismic wavelets and the seismic polarity are not available. In this study, using subsurface (i.e., 2D seismic profiles) data related to the Marine Zones B, D and F (offshore Puglia) a review of the basic pulse shape and polarity of seismic wavelets, as well as the shape and polarity of principal reflectors has been addressed. Moreover, borehole data (i.e., lithology and sonic logs) have been used to identify abrupt average velocity changes linked to different lithostratigraphic successions recorded as dominant high-amplitude reflectors.

KEY-WORDS: seismic pulse shape and polarity, ViDEPI project, offshore Puglia, velocity analysis, seismic profiles interpretation.

INTRODUCTION

The Visibility of Petroleum Exploration Data in Italy (ViDEPI) project, related to hydrocarbon exploration activities performed in Italy, is the largest and public database in the Mediterranean area including seismic profiles and exploration well logs. The project contains data surveyed since 1957, made available by the Ministry for the Economic Development of the Italian Government. The database is accessible since 2007 on the website www.videpi.com, where analogic scanned documents having a PDF format are available to be freely downloaded (ViDEPI, 2015). Seven Marine Zones, named from A to G, includes the seismic profiles acquired offshore the Italian Peninsula (Fig. 1a). In detail, the dataset discussed in the present study is located in the Adriatic and Ionian seas, offshore the Puglia administrative regional territory (hereinafter Puglia), within the Marine Zones B, D and F (Fig. 1b).

The seismic lines pertaining to the Marine Zones B and D were acquired in the late 1960s, and the ones falling into the Marine Zone F were obtained during mid-1970s. The releasing of these subsurface data gave, in the recent years, a significant impulse to the research activity on the tectono-sedimentary evolution of the Mesozoic Apulia Platform and its adjacent basins. It also helped to highlight the involvement of this sector of the Adria Plate in the Dinarides-Hellenides (to the East) and Apennines (to the West) orogenic systems during Cenozoic (Figs. 1a, c) (Nicolai & Gambini, 2007; Scisciani & Calamita, 2009; Del Ben et al., 2010, 2015; Santantonio et al., 2013; Festa et al., 2014, 2019a, b; Pace et al., 2015; Volpi et al., 2015; Teofilo et al., 2016, 2018; Milia et al., 2017a, b; Maesano et al., 2020; Cicala et al., 2021, 2022b; Chizzini et al., 2022; Pellen et al., 2022). The importance of the vintage seismic profiles has also been recently underlined by Brancatelli et al. (2022), Cicala et al. (2022a) and Conti et al. (2022). In particular, the present paper represents an upgrade, with an implementation concerning the velocity analysis, of the first attempt by Cicala et al. (2022a) on the recognition of shape and polarity of the seismic pulses, that were missing information on the

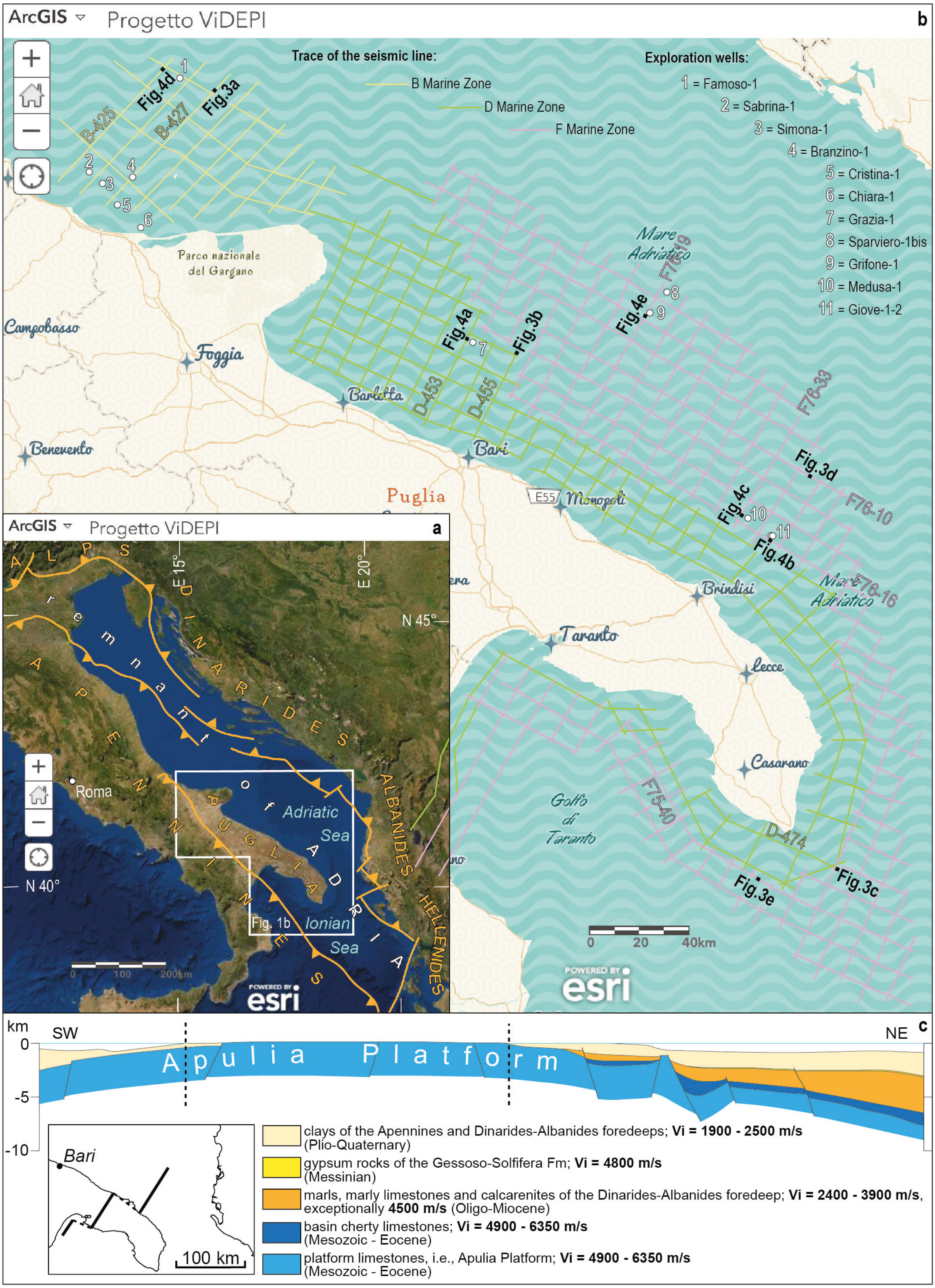

Fig. 1 - (a) Structural sketch map illustrating the remnant of Adria surrounded by Alps, Apennines and Dinarides-Albanides-Hellenides orogenic belts (modified after Cicala et al., 2021); basemap modified after ViDEPI (2015). (b) Map of the Puglia and surrounding (see Fig. 1a for the location) exhibiting the traces of seismic lines and the location of exploration wells provided of sonic logs falling within the B, D and F Marine Zones (modified after ViDEPI, 2015). (c) Schematic regional geological cross section from the Apennines foredeep to the Dinarides-Albanides foreland basin (redrawn and simplified after Fantoni & Franciosi, 2010); interval velocities (Vi), estimated by available sonic logs, are indicated.

seismic lines in the offshore the Puglia. Moreover, Brancatelli et al. (2022) have reprocessed with today's standard techniques some seismic data acquired during the 1970s, as part of other projects (e.g., the Mediterranean Sea project, conducted between 1969 and 1982 by the National Institute of Oceanography and Applied Geophysics, OGS, of Trieste, Italy) in the offshore the Puglia leading to an improvement of their quality and resolution.

However, seismic data in the offshore the Puglia, as well as the entire seismic database of the ViDEPI project, present several limitations. As a matter of fact, the standard processing procedure applied (Yilmaz, 2001), led to unmigrated seismic profiles, missing basic information for a geological interpretation as accurate as possible. In addition, the basic shape of the seismic wavelets and the seismic polarity information are very difficult to visualize due to the graphic rendering low resolution, as well as to the poorly processed seismic data. Nevertheless, in several cases the reflectors are quite clearly visible, giving the chance to make considerations on the polarity of the seismic wavelets, and, consequently, to interpret as correctly as possible, the position of some geological boundaries.

Therefore, the main objective of the present contribution is to provide a method to obtain the shape and polarity of the seismic wavelets and geological meaning of the principal reflectors shown by the vintage seismic lines from the Marine Zones B, D and F in the offshore the Puglia. With this aim, the sonic logs were functional to identify sudden P-waves interval velocity variations occurring among distinct lithostratigraphic successions. The used methodological approach and the achieved results are preparatory for future research studies expecting to interpret vintage seismic lines, the latter not necessarily restricted to the offshore the Puglia.

AN OUTLINE OF THE BASIC SHAPE AND POLARITY OF SEISMIC PULSES

The pulse shape assessment of the seismic wavelet is a pivotal step for the interpretation of seismic profiles (e.g., Badley, 1987; Veeken & van Moerkerken, 2013). The seismic pulses represented on seismic profiles can be of two different main types: (I) minimum-phase and (II) zero-phase. The minimum-phase pulse includes a succession of waves in a damped sinusoidal trend with depth, with the wavelet onset indicating the acoustic impedance boundary (Figs. 2a-d). Differently, the zero-phase pulse consists of a succession of waves in a symmetrically damped sinusoidal trend, consisting in lower amplitudes waves on the sides of a central higher amplitude wave; the crest of this latter principal wave is considered indicating the acoustic impedance boundary (Figs. 2e-h). It is worth mentioning that the peak and trough represent the wave on right and left of the wiggle line, respectively, and that the area enveloped by the peak is conventionally filled in black (Fig. 2).

The wavelet polarity is a conventional display of the sudden variation of the reflection coefficient, and it changed over the time based on different conventions. According to the latest standards released by the Society of Exploration Geophysicists (SEG) (Sheriff, 2002), normal and reverse polarities are defined under the condition where the acoustic impedance increases sharply with depth. Therefore, the normal polarity is given by the onset (i) of a trough within the minimum-phase pulse (Fig. 2a), and (ii) of the higher peak of the zero-phase wavelet (Fig. 2e). Conversely, the reverse polarity is characterized by the onset (iii) of a peak within the minimum-phase wavelet (Fig. 2b), and (iv) of the higher trough of the zero-phase pulse (Fig. 2f) (Sheriff, 2002). However, it should be noted that in the North Sea, as well as few other areas, the convention regarding the zero-phase pulse is reversed (Sheriff, 2002; Veeken & van Moerkerken, 2013), i.e., the normal polarity given by the higher trough (Fig. 2f), and the reverse one characterized by the main peak (Fig. 2e).

Under the condition where the acoustic impedance decreases sharply with depth, the normal polarity is defined by the onset of a peak within the minimum-phase wavelet (Fig. 2c), and the higher trough of the zero-phase pulse (Fig. 2g) (e.g., Badley, 1987). Accordingly, the reverse polarity would be given by the opposite situation (Figs. 2d, h).

The seismic lines preceding the last update of the SEG standards (Sheriff, 2002), often follow different displaying of the wavelet shape and polarity (Veeken & van Moerkerken, 2013). To make everything more challenging, pulse shape and polarity are missing information for legacy seismic profiles acquired in the Marine Zone B, D and F (ViDEPI, 2015) (Fig. 1b). As a result, the following issues can cause misinterpretation of some seismic records:

- The minimum-phase normal polarity due to abrupt increase of acoustic impedance with the depth (Fig. 2a) is the same of the minimum-phase reverse polarity resulting from sudden decrease of acoustic impedance with the depth (Fig. 2d),
- the minimum-phase reverse polarity due to abrupt increase of acoustic impedance with the depth (Fig. 2b) is the same of the minimum-phase normal polarity resulting from sudden decrease of acoustic impedance with the depth (Fig. 2c),
- the zero-phase normal polarity due to abrupt increase of acoustic impedance with the depth (Fig. 2e) is the same of the zero-phase reverse polarity resulting from sudden decrease of acoustic impedance with the depth (Fig. 2h),
- the zero-phase reverse polarity due to abrupt increase of acoustic impedance with the depth (Fig. 2f) is the same of the zero-phase normal polarity resulting from sudden decrease of acoustic impedance with the depth (Fig. 2g).

FROM WAVELETS TO PATTERNS OF REFLECTORS TO IDENTIFY THE PULSE SHAPE AND POLARITY

With the aim to assess the enigmatic display convention for the pulse shape and polarity of the seismic contained in the ViDEPI project, the seismic wavelet resulting at the sea floor/sea water interface is an unequivocal record of the sudden increase of the acoustic impedance. In the examples shown in Figure 2 (i.e., a, b, e, f), we have reconstructed by the lateral juxtaposition of the default seismic wavelets (minimum-phase and zero phase with both normal and reverse polarity) the theoretical pattern of reflectors expected at this interface: only one of these four possibilities represents the wavelet shape and polarity sought. Hence, we suggest that the comparison of these four cases (Fig. 2a, b, e, f) with the patterns of reflectors directly visible on the seismic profile (especially at the

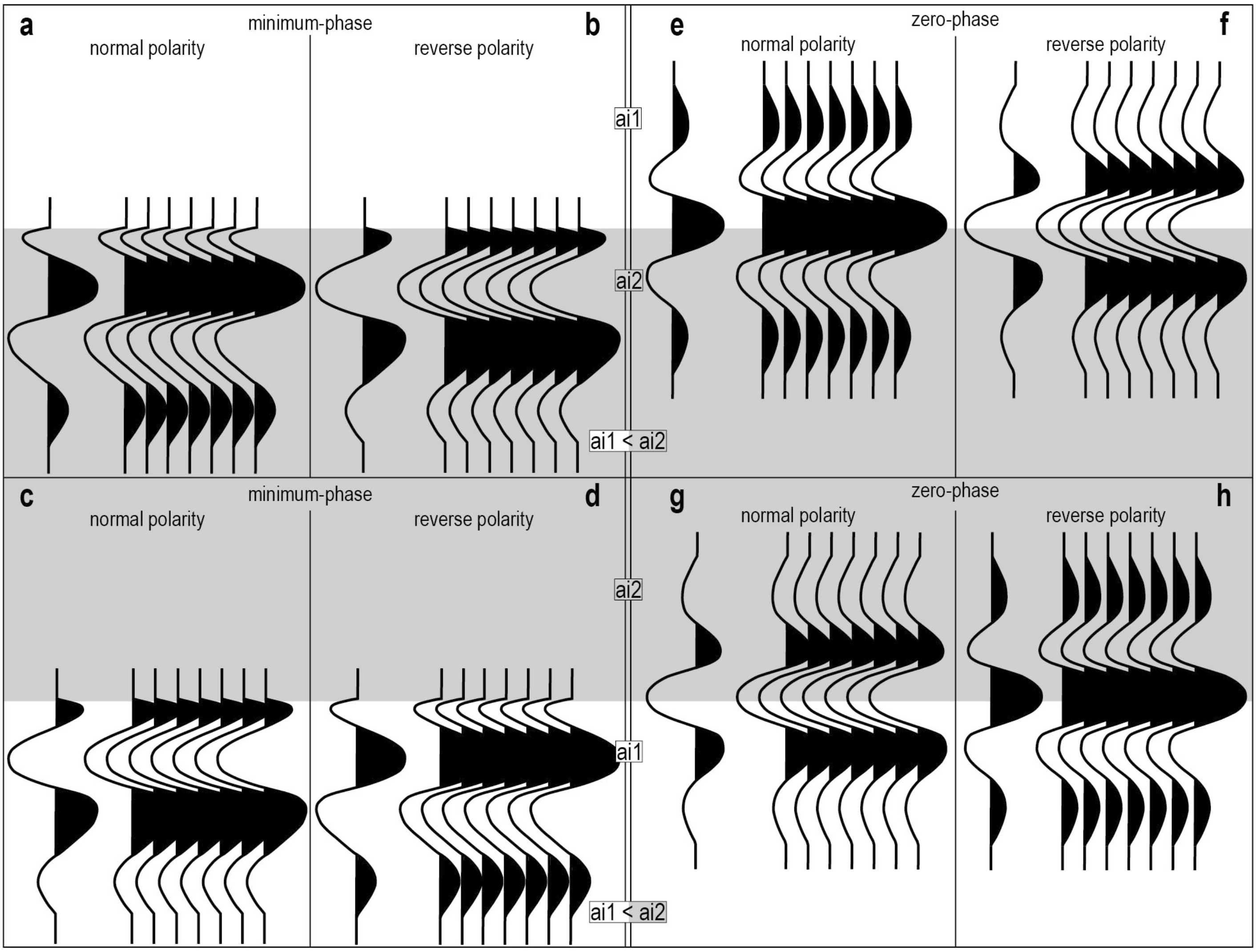

Fig. 2 - (a-h) On left of each frame, possible cases of basic seismic wavelet and polarity for a single pulse related to sudden variation with depth of acoustic impedance; ai = acoustic impedance. (a, b, e, f) On right of each frame, reconstruction of theoretical patterns of reflectors resulting from the net increase with depth of acoustic impedance. (c, d, g, h) On right of each frame, reconstruction of theoretical patterns of reflectors resulting from the net decrease with depth of acoustic impedance.

sea water/sea floor interface) may give strong indications on the correct wavelet shape and polarity.

By applying the proposed approach to the legacy seismic profiles selected for this study (Fig. 1b), a zero-phase normal polarity (Fig. 2e) is strongly suggested for the seismic lines falling within Marine Zone B (Fig. 3a). As shown, the zero-phase normal polarity is characterized by peaks strong reflector symmetrically sided downward and upward by troughs both theoretically (Fig. 2e) and at the sea water/sea floor interface (Fig. 3a). Accordingly, the seafloor should be traced in the middle of the peaks composing the strong reflector (Fig. 3a).

The analysis seems a bit more complex when applied to the seismic lines belonging to the Marine Zone D, where the reflectors pattern at the sea water/sea floor interface may reflects both zero-phase normal polarity (Figs. 2e, 3b) and zero-phase reverse polarity (Figs. 2f, 3c). In fact, some seismic lines show a pattern of two strong peaks reflectors separated by troughs (Fig. 3c), that should typically characterize the zero-phase reverse polarity (Fig. 2f). Accordingly, the seafloor could be traced both in the middle of the strong reflector made by peaks (Fig. 3b), otherwise in the middle of the troughs (Fig. 3c).

Finally, for the seismic profiles of the Marine Zone F, the sudden increase of acoustic impedance (Fig. 2) suggests a zero-phase reverse polarity (Figs. 2f, 3d, e). Accordingly, the seafloor should be traced in the middle of the troughs (Figs. 3d, e).

Ultimately, the interpretation of such seismic lines (e.g., Fig. 4a-e) should necessarily consider the pattern of reflectors dealing with the sea water/sea floor interface to reveal the wavelet shape and the polarity. As partially shown in Figure 2, the major rapid acoustic impedance change should comply with the reconstructed theoretical patterns of reflectors at the related interfaces at depth (e.g., Fig. 4a-e). Therefore, in addition to the four a, b, e, f cases (Fig. 2), we have also considered the sudden acoustic impedance decrease with depth, although less common in the study area, by reconstructing the reflectors patterns in the four c, d, g, h frames: normal and reverse polarity for both the minimum-phase shape wavelet (Figs. 2c, d), and the zero-phase pulse (Figs. 2g, h). Concerning the vintage legacy seismic lines of

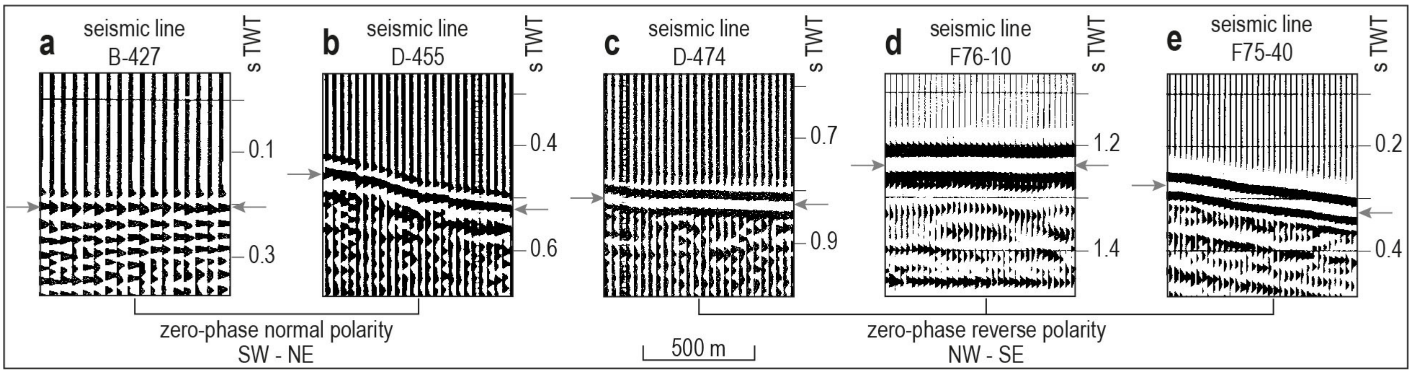

Fig. 3 - (a-e) Portions of some seismic lines from the B, D and F Marine Zones offshore the Puglia (Fig. 1b for the location) exhibiting the patterns of the reflectors resulting from the sea water/sea floor interface, the latter pointed by greyish arrows.

the offshore the Puglia B, D and F marine zones (ViDEPI, 2015), the recognition, through the patterns of reflections, of abrupt increasing or decreasing of acoustic impedance with depth should be limited to the zero-phase pulse, with both normal and reverse polarity (Figs. 2e-h).

VELOCITY ANALYSIS

To explore the seismic response of major geological boundaries in depth, we have employed exploration wells logs. The analysis of sonic logs available for some exploration wells drilled in the offshore the Puglia (i.e., Sabrina-1, Simona-1, Cristina-1, Branzino-1, Famoso-1, Chiara-1, Grazia-1, Grifone-1, Medusa-1, Giove-1-2 and Sparviero-1bis; Fig. 1b for the location), allowed us to estimate the P-waves average velocity for the Plio-Pleistocene clay-dominated succession, the Messinian gypsum rocks of the Gessoso-Solfifera Fm, the Oligo-Miocene interval, mainly composed of marls, marly limestones and calcarenites, and the Mesozoic-Eocene platform limestones or basin cherty limestones (Fig. 1c). According to Rider (2002), an average value of the interval transit time, Δt_{av}, which is the inverse of the average of the interval velocity, $V_{av} = 1/\Delta t_{av}$, can be graphically obtained for each of the above stratigraphic bodies, from the sonic logs. The unit of measurement of the interval transit time, hence of Δt_{av}, is µs/ft, where µs is microseconds and ft is feet. In the two examples of Figures 4f, g, concerning the Giove1-2 and Branzino-1 exploration wells, Δt_{av} = 158 µs/ft, Δt_{av} = 68 µs/ft and Δt_{av} = 61 µs/ft have been obtained for the Plio-Pleistocene clay-dominated succession, the Oligo-Miocene interval mainly consisting of calcarenites, and the Upper Cretaceous platform limestones, respectively. Moreover, in the further two examples presented in Figures 4h and 4i related the Famoso-1 and Grifone-1 wells, Δt_{av} = 63 µs/ft and Δt_{av} = 60 µs/ft have been evaluated for the Messinian deposits of the Gessoso-Solfifera Fm. and the Lower Cretaceous basinal cherty limestones, respectively. In the next step, the average velocity $1/\Delta t_{av}$ has been calculated and converted to the velocity m/s (m = meters, s = seconds), considering that µs = 10^{-6}s, and ft = 0.3048 m (Rider, 2002). Therefore, taking into account all the available sonic logs, the following average velocities, V_{av}, ranges have been estimated for the drilled stratigraphic bodies in the offshore Puglia: 1900-2500 m/s for the Plio-Pleistocene succession, 4800 m/s for the Gessoso-Solfifera Fm, 2400-3900 m/s (extraordinarily 4500 m/s in the Giove-1-2 exploration well) for the Oligo-Miocene interval, and 4900-6350 m/s for the Mesozoic-Eocene units (Figs. 1c, 4a-e). It should be noted that the evaluated average velocities are in line with those reported by Morelli (2002) and Teofilo et al. (2018) for the same lithotypes present in the subsurface offshore Puglia.

MAIN GEOLOGICAL BOUNDARIES, ABRUPT VARIATIONS OF AVERAGE VELOCITY AND REFLECTORS PATTERNS

Unfortunately, due to the poor processing of the seismic data and their low definition in the graphic rendering of the seismic profiles, the reflectors resulting from the average velocity sudden variations are not always clearly visible. However, these patterns of reflectors can be recognised because of other peculiar features.

From the top, the first evident velocity variation with the depth is represented by a sudden increase related to the sharp transition between the Plio-Pleistocene succession and the below Oligo-Miocene interval (e.g., Fig. 4a-f). For the marine zones D and F, the correlation among the exploration wells Grazia-1, Giove-1-2, and Medusa-1 and the seismic profiles D-453, F76-16, and F76-33, respectively (Fig. 1b), exhibits the Plio-Pleistocene/Oligo-Miocene interface marked by well-developed troughs characteristically sided downward and upward by peaks reflectors (Figs. 2e, 4a-c). As shown, this seismic response is consistent with the zero-phase reverse polarity of the reflectors pattern resulting from the sea water/sea floor interface (Figs. 4a-c).

Data from Marine Zone B is suitable for the investigation of the seismic response to Plio-Pleistocene clays/Gessoso-Solfifera Fm interface, by means of correlation between the available sonic logs of Sabrina-1, Simona-1, Branzino-1, Famoso-1 exploration wells (Fig. 1b, for their location) and seismic profiles. It should be noted that the Gessoso-Solfifera Fm generally show a relatively small thickness up to 110 m, the latter recorded in the Famoso-1 exploration well (Fig. 4d). Since for the seismic lines falling within the Marine Zone B the zero-phase normal polarity has been inferred (e.g., Figs. 3a, 4d), the Plio-Pleistocene clays/Gessoso-Solfifera Fm interface is effectively represented by an evident reflector made of peaks sided by troughs (Figs. 2e, 4d). Deeper, the subsequent rapid decrease of the velocity coincides with the sharp transition from

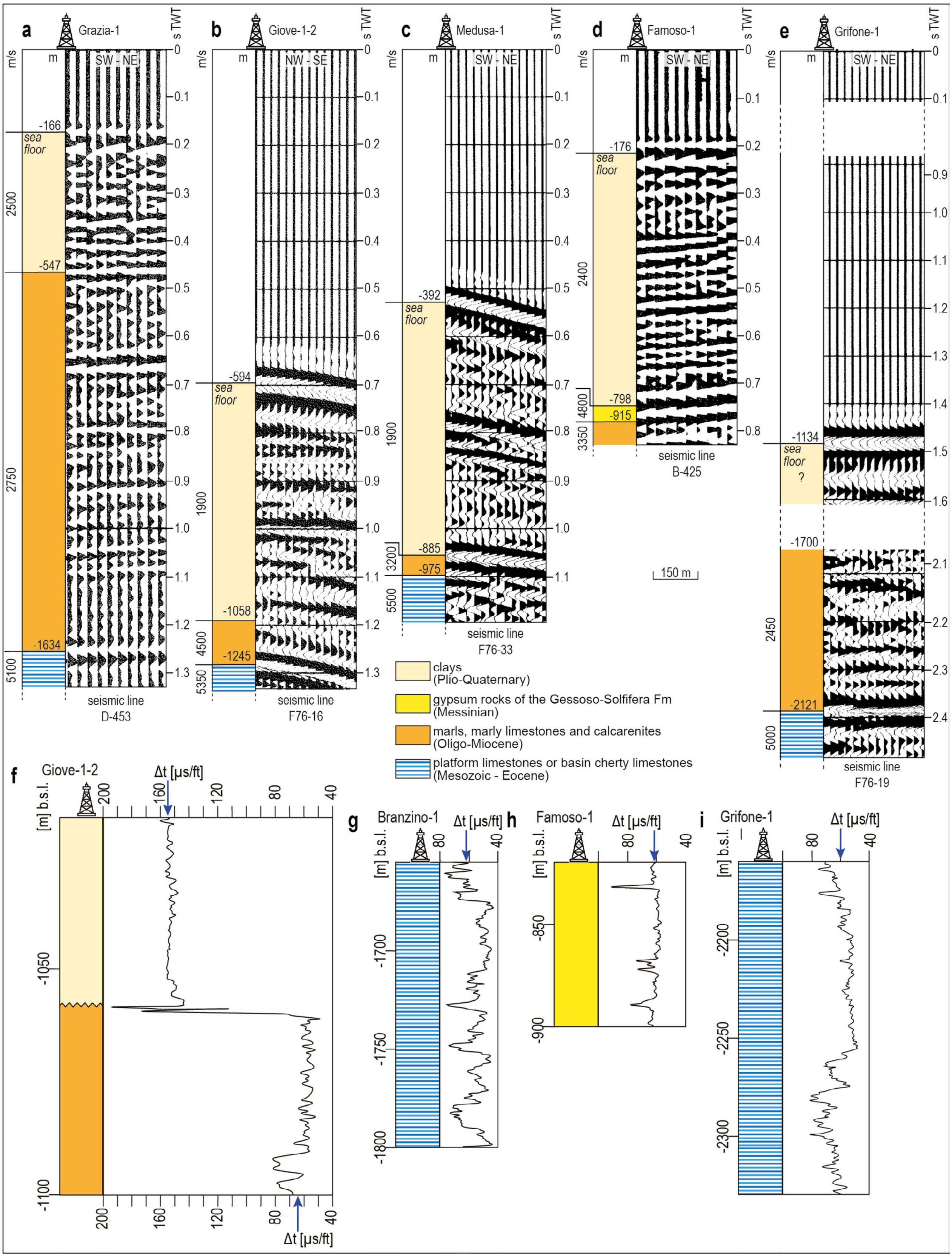

Fig. 4 - (a-e) Parts of seismic lines correlated with lithostratigraphic log of exploration wells within the B, D and F Marine Zones offshore Puglia (Fig. 1b for the location), exhibiting the main reflections resulting from interval velocity sudden increases with depth at lithostratigraphic successions interfaces. The horizontal bar, of 150 m, refers to the parts of the seismic lines. (f) Portion of lithostratigraphic and sonic log of the Giove1-2 exploration wells; the sonic log is characterized by a sudden increase of interval velocity at the interface among the Plio-Pleistocene clay-dominated interval, above, and Oligo-Miocene calcarenites succession, below. (g) Portion of lithostratigraphic and sonic log of the Branzino-1 well (Fig. 1b for the location), characterized by Upper Cretaceous platform limestones. (h) Portion of lithostratigraphic and sonic log of the Famoso-1 well (Fig. 1b for the location), characterized by gypsum rocks of the Gessoso-Solfifera Fm. (i) Portion of lithostratigraphic and sonic log of the Grifone-1 well (Fig. 1b for the location), characterized by Lower Cretaceous basin cherty limestones. The average of the interval transit time, Δtav, graphically obtained as average value from the sonic logs, is pointed by arrows in the figures f-i.

the Gessoso-Solfifera Fm to the below Miocene marls and marly limestones (Fig. 4d). However, the expected seismic signal to this abrupt velocity decrease (e.g., Fig. 2g) is practically undetectable on the seismic profiles due to the typical relatively small thickness of the Gessoso-Solfifera Fm. Accordingly, the seismic signal could be masked by the strong reflection related to the above Plio-Pleistocene clays/Gessoso-Solfifera Fm interface.

A further key feature recognizable in seismic profile is the sharp transition to the Mesozoic-Eocene platform and basins carbonate rocks characterized by the higher interval velocity (Fig. 1c). In particular, the rapid increase of average velocity from the Oligo-Miocene interval to the Mesozoic-Eocene basin carbonates is evidenced by the sonic logs of the Grazia-1 and Grifone-1 exploration wells, intercepting the seismic lines D-453 and F76-19, respectively (Fig. 1b). These seismic profiles are characterized by zero-phase reverse polarity resulting from the pattern of reflectors related to the sea water/sea floor interface (Figs. 4a, e). Accordingly, the top of the Mesozoic-Eocene basin carbonates is marked by evident troughs sided downward and upward by strong peaks reflectors (e.g., Fig. 2f), as observable in the seismic lines D-453 (Fig. 4a) and F76-19 (Fig. 4e). Similarly, the top of the Mesozoic-Eocene platform limestones is characterized by evident troughs sided downward and upward by strong peaks reflectors (e.g., Figs. 2f, 4c), as shown by the correlation among the seismic profile F76-33 and the Medusa-1 exploration well (Fig. 1b). Actually, the seismic reflection pattern is consistent with the zero-phase reverse polarity derived from the reflectors at the sea water/sea floor interface (Fig. 4c). Furthermore, the sharp increase of interval velocity due to the presence of the Mesozoic-Eocene platform limestones can be also inferred from the sonic logs of Simona-1, Sabrina-1, Chiara-1 and Famoso-1 exploration wells (Fig. 1b). However, in the seismic lines intercepting Simona-1, Sabrina-1 and Famoso-1 exploration wells, the seismic signal of the Gessoso-Solfifera Fm masks the reflection of the below top of the Mesozoic-Eocene platform limestones. Unfortunately, the correlation between the Chiara-1 exploration well and the nearest seismic line (Marine Zone B) would be problematic due to the large distance (about 10 km) among them.

CONCLUDING REMARKS

The analysis of subsurface data (i.e., 2D seismic lines, lithology and sonic logs) from the Marine Zones B, D and F offshore Puglia points towards the following major results:

i. The seismic pulse recorded at the sea floor represents an abrupt increase of the acoustic impedance with depth at the sea water/sea floor interface. Accordingly, the comparison between reconstructed theoretical reflectors expected at the acoustic impedance boundary and the pattern of the reflectors visible in the ViDEPI seismic lines (where this information is not available) can help to recognize the correct wavelet shape and polarity,
ii. the seismic profiles related to the Marine Zone B are characterised by zero-phase normal polarity. The identification of the basic shape of the seismic pulses and the seismic polarity results more difficult for the Marine Zone D profiles because different seismic lines show sea water/sea floor interface comparable with both a zero-phase normal polarity or a zero-phase reverse polarity. Accordingly, a bespoke analysis of the seismic pulse at the sea floor should be made for each seismic profile. Finally, a zero-phase reverse polarity have been revealed for the Marine Zone F seismic lines,
iii. the analysis of the available sonic logs allows the extrapolation of the average velocities of the Plio-Pleistocene clay-dominated interval (1900-2500 m/s), the Messinian gypsum rocks of the Gessoso-Solfifera Fm (4800 m/s), the Oligo-Miocene succession mainly composed of marls, marly limestones and calcarenites (2400-3900 m/s and exceptionally 4500 m/s), and the Mesozoic-Eocene platform carbonates or basin cherty limestones (4900-6350 m/s).

ACKNOWLEDGEMENTS

We are grateful to two anonyms Reviewers who helped us to improve the manuscript. This work has been financially supported by the PhD in Geosciences grant of the Università degli Studi di Bari “Aldo Moro”, to Marianna Cicala, and by the following research funds, to Vincenzo Festa: Progetto “GeoSciences: un’infrastruttura di ricerca per la Rete Italiana dei Servizi Geologici - GeoSciences IR” (codice identificativo domanda: IR0000037); CUP: I53C22000800006. Piano Nazionale di Ripresa e Resilienza, PNRR, Missione 4, Componente 2, Investimento 3.1, “Fondo per la realizzazione di un sistema integrato di infrastrutture di ricerca e innovazione” finanziato dall’Unione Europea – Next Generation EU.

REFERENCES

Badley M.E. (1987) - Practical Seismic Interpretation. International Human Resources Development Corp., Boston, 266 pp.

Brancatelli G., Forlin E., Bertone N., Del Ben A. & Geletti R. (2022) - Time to depth seismic reprocessing of vintage data: a case study in the Otranto Channel (South Adriatic Sea). In: Bell R., Iacopini D., Vardy M. (eds.), Interpreting Subsurface Seismic Data. Elsevier, 157-197, https://doi.org/10.1016/B978-0-12-818562-9.00009-1.

Chizzini N., Artoni A., Torelli L., Basso J., Polonia A. & Gasperini L. (2022) - Tectono-stratigraphic evolution of the offshore Apulian Swell, a continental sliver between two converging orogens (Northern Ionian Sea, Central Mediterranean). Tectonophysics, 839, 229544, https://doi.org/10.1016/j.tecto.2022.229544.

Cicala M., Chiarella D., De Giosa F. & Festa V. (2022a) - Conventional data display and implications for the interpretation of seismic profiles: a discussion on the ViDEPI seismic database offshore Apulia (southern Italy). Arab. J. Geosci., 15, 395, https://doi.org/10.1007/s12517-022-09721-z.

Cicala M., Festa V. & Marrone A. (2022b) - Data extraction from vintage well sonic log graphs in the ViDEPI project (offshore the Apulia, southern Italy): A multi-useful dataset. Data in Brief, https://doi.org/10.1016/j.dib.2022.108814.

Cicala M., Festa V., Sabato L., Tropeano M. & Doglioni C. (2021) - Interference between Apennines and Hellenides foreland basins around the Apulian swell (Italy and Greece). Mar. Petrol. Geol., 133, 105300, https://doi.org/10.1016/j.marpetgeo.2021.105300.

Conti A., Maffucci R. & Bigi S. (2022) - The use of public vintage seismic reflection profiles. In: Bell R., Iacopini D., Vardy M. (eds.), Interpreting Subsurface Seismic Data. Elsevier, 127-156, https://doi.org/10.1016/B978-0-12-818562-9.00003-0.

Del Ben A., Geletti R. & Mocnik A. (2010) - Relation between recent tectonics and inherited Mesozoic structures of the central-southern Adria plate. B. Geofis. Teor. Appl., 51, 99-115.

Del Ben A., Mocnik A., Volpi V. & Karvelis P. (2015) - Old domains in the South Adria plate and their relationship with the West Hellenic front. J. Geodyn., 89, 15-28, https://doi.org/10.1016/j.jog.2015.06.003.

Fantoni R. & Franciosi R. (2010) - Tectono-sedimentary setting of Po Plain and Adriatic foreland. Rend. Lincei-Sci. Fis., 21, 197-209, https://doi.org/10.1007/s12210-010-0102-4.

Festa V., De Giosa F., Moretti M., Del Gaudio V. & Pierri P. (2019a) - In search of the seismogenic fault of the March 23rd 2018 earthquake (Mw 3.7) near Brindisi (Puglia, Southern Italy). Geol. Croat., 72, 137-144, https://doi.org/10.4154/gc.2019.10.

Festa V., Fregola R.A., Acquafredda P., De Giosa F., Monno A. & Ventruti G. (2019b) - The enigmatic ascent of Ca-sulphate rocks from a deep dense source layer: evidences of hydration diapirism in the Lesina Marina area (Apulia, southern Italy). Int. J. Earth Sci., 108, 1897-1912, https://doi.org/10.1007/s00531-019-01739-1.

Festa V., Teofilo G., Tropeano M., Sabato L. & Spalluto L. (2014) - New insights on diapirism in the Adriatic Sea: The Tremiti salt structure (Apulia offshore, Southeastern Italy). Terra Nova, 26, 169-178, https://doi.org/10.1111/ter.12082.

Maesano F.E., Volpi V., Civile D., Basili R., Conti A., Tiberti M.M., Accettella D., Conte R., Zgur F. & Rossi G. (2020) - Active Extension in a Foreland Trapped Between Two Contractional Chains: The South Apulia Fault System (SAFS). Tectonics, 39, e2020TC006116, https://doi.org/10.1029/2020TC006116.

Milia A., Iannace P. & Torrente M.M. (2017a) - Active tectonic structures and submarine landslides offshore southern Apulia (Italy): A new scenario for the 1743 earthquake and subsequent tsunami. Geo-Mar. Lett., 37, 229-239, https://doi.org/10.1007/s00367-017-0493-7.

Milia A., Torrente M.M. & Iannace P. (2017b) - Pliocene-Quaternary orogenic systems in Central Mediterranean: The Apulia-Southern Apennines-Tyrrhenian Sea example. Tectonics, 36, 1614-1632, https://doi.org/10.1002/2017TC004571.

Morelli D. (2002) - Evoluzione tettonico-stratigrafica del Margine Adriatico compreso tra il Promontorio garganico e Brindisi. Mem. Soc. Geol. It., 57, 343-353.

Nicolai C. & Gambini R. (2007) - Structural architecture of the Adria platform-and-basin system. Boll. Soc. Geol. It., Suppl. 7, 21-37.

Pace P., Scisciani V., Calamita F., Butler R.W.H., Iacopini D., Esestime P. & Hodgson N. (2015) - Inversion structures in a foreland domain: Seismic examples from the Italian Adriatic Sea. Interpretation, 3, SAA161–SAA176, https://doi.org/10.1190/INT-2015-0013.1.

Pellen R., Aslanian D., Rabineau M., Suc J.-P., Cavazza W., Popescu S.-M. & Rubino J.-L. (2022) - Structural and sedimentary origin of the Gargano - Pelagosa gateway and impact on sedimentary evolution during the Messinian Salinity Crisis. Earth-Sci. Rev., 232, 104114, https://doi.org/10.1016/j.earscirev.2022.104114.

Rider M. (2002) - The geological interpretation of well logs. Rider-French Consulting Ltd., Sutherland, 280 pp.

Santantonio M., Scrocca D. & Lipparini L. (2013) - The Ombrina-Rospo Plateau (Apulian Platform): Evolution of a Carbonate Platform and its Margins during the Jurassic and Cretaceous. Mar. Petrol. Geol., 42, 4-29, https://doi.org/10.1016/j.marpetgeo.2012.11.008.

Scisciani V. & Calamita F. (2009) - Active intraplate deformation within Adria: Examples from the Adriatic region. Tectonophysics, 476, 57-72, https://doi.org/10.1016/j.tecto.2008.10.030.

Sheriff R. (2002) - Encyclopedic dictionary of applied geophysics. Society of Exploration Geophysicists, Tulsa, 442 pp.

Teofilo G., Antoncecchi I. & Caputo R. (2018) - Neogene-Quaternary evolution of the offshore sector of the southern Apennines accrectionary wedge, Gulf of Taranto, Italy. Tectonophysics, 378-379, 16-32, https://doi.org/10.1016/j.tecto.2018.05.006.

Teofilo G., Festa V., Sabato L., Spalluto L. & Tropeano M. (2016) - 3D modelling of the Tremiti salt diapir in the Gargano offshore (Adriatic Sea, southern Italy): constraints on the Tremiti Structure development. Ital. J. Geosci., 135, 474-485, https://doi.org/10.3301/IJG.2015.40.

ViDEPI (2015) - Visibilità dei dati afferenti all'attività di esplorazione petrolifera in Italia. https://www.videpi.com.

Veeken P. & van Moerkerken B. (2013) - Seismic Stratigraphy and Depositional Facies Models. EAGE Publications bv, Houten, 494 pp.

Volpi V., Forlin F., Donda F., Civile D., Facchin L., Sauli S., Merson B., Sinza-Mendieta K. & Shams A. (2015) - Southern adriatic sea as a potential area for CO2 geological storage. Oil Gas Sci. Technol., 70, 713-728, https://doi.org/10.2516/ogst/2014039.

Yilmaz Ö. (2001) - Seismic data analysis: processing, inversion, and interpretation of seismic data. In: Doherty S.M. (ed.), Investigation in Geophysics. Society of Exploration Geophysicists, 2027 pp.